In-house low-cost water table prototype to practically analyse the modelling compressible flow in a fluid engineering course

Sílvia Armengol, Gustavo Raush, Pedro J Gamez-Montero

Abstract

The present work studies the hydro-gasdynamic analogy between a shock wave, occurring in supersonic internal or external compressible flows, and a hydraulic jump, a sort of normal shock occurring in open-channel flows. It consists of an extensive theoretical framework followed by a practical analysis, the aim of which was to experimentally trigger the hydraulic jump, both normal and oblique, while using a low-cost designed lab prototype. The assembly development, called "water table", arises from the necessity of economical alternatives to expensive supersonic wind tunnels in the experimental study of compressible fluid dynamics. With this objective in mind, a hydraulic canal based on a Laval nozzle was constructed where water flow could accelerate from subcritical to critical to supercritical regime and then return to subcritical regime through a hydraulic jump. In addition, multiple design alternatives were evaluated considering environmental, economic, functional and aesthetics factors. A low-cost implementation was the critical criterion in the design process. The measurements have revealed that the geometry of the nozzle and the wedges designed as obstacles to cause obliquity are the most significant and influential elements in the formation of a hydraulic jump in the experimental set-up. Regarding the experimental variables, the experiments demonstrate the effect of the upstream and downstream heights of the hydraulic jump in the data collection. This experience is a step forward in supporting students in the understanding of compressible flow and its principles by providing an in-house experimental set-up that promotes active learning, motivation and interest in fluid mechanics.

Keywords

Introduction

The experimental study of compressible flow dynamics has been of growing interest since the 1940s, for both experts and students of fluid mechanics. There are a wide range of distinguished works and books, from Shapiro[1] (1953) to Anderson[2] (2003). Unfortunately, the experimental simulation of this type of flow presents the disadvantage of requiring expensive equipment such as a supersonic wind tunnel that not all universities can afford[3,4].

The main objective of this article is to offer a description of the design and manufacture of an experimental equipment that can show the theory behind compressible flow, while collecting

Department of Fluid Mechanics, Universitat Politecnica de Catalunya, Campus Terrassa, Terrassa, Spain

Corresponding author:
Pedro J Gamez-Montero, IAFARG, Department of Fluid Mechanics, Universitat Politecnica de Catalunya, Campus Terrassa, Terrassa, Spain
Email: pedro.javier.gamez@upc.edu

data from an incompressible flow like water. The purpose is to illustrate this concept by its hydro-gasdynamic analogy with the hydraulic jump, since it shows similar characteristics of a shock wave and can be easily and economically reproduced.

This analogy has long been investigated; scientists such as Mach or Von Karman presented the first works, gaining popularity within the field. Thus, research focused on this topic is still of interest today in universities[5-7]. The goal of this work is not only to show the evidence of theoretical formulas while experimenting, but also to develop it through an inexpensive and easy-to-manufacture experimental assembly; in other words, an in-house ad-hoc low-cost water table.

Theoretical framework

The purpose of the theoretical framework is to elucidate the analogy between the dimensionless Mach (Ma) and Froude (Fr) numbers because they are both based on describing the fluid velocity, compressible and incompressible flow, respectively. First, it is necessary to establish the following assumptions in order to conduct a correct analysis[8] and they are described in Table 1.

Table 1. Assumptions and approximations

Air	Water
i. Ideal gas and compressible flow	ii. Incompressible flow
iii. Steady-state and unidimensional flow	iii. Steady-state and unidimensional flow
iv. Isoenergetic flow and outside the boundary layer	iv. Isoenergetic flow and outside the boundary layer
v. Adiabatic and isentropic flow – except when crossing a shock wave	vi. Negligible surface tension effects
vii. Constant ratio of specific heat capacities (γ)	viii. Negligible viscous effect

Numbers Ma and Fr analogy

Any streamtube in a compressible flow, like air, satisfies the steady-state conservation of energy equation[9],

$$h_1 + \frac{1}{2}u_1{}^2 + gz_1 = h_2 + \frac{1}{2}u_2{}^2 + gz_2 - q + w_v \tag{1}$$

where subindex 1 indicates upstream and subindex 2 downstream, h is the specific enthalpy, u the fluid velocity, g gravity, z the height from a reference point, q heat transfer and w_v work. The terms of potential energy in a gas are very small compared to the kinetic and enthalpic ones and that is why they can be neglected. In addition, the terms q and w_v can be neglected due to the assumptions presented in Table 1.

The enthalpy from equation (1) corresponds to the maximum that a fluid can acquire when it is driven to rest adiabatically, called stagnation enthalpy (h_0)[9],

$$h + \frac{1}{2}u^2 = h_0 = ct. \tag{2}$$

According to the assumptions i) and v), the enthalpy of an isentropic flow of an ideal gas is defined by the product of its specific heat at constant pressure (c_p) and its temperature (T). Therefore, equation (2) can be rewritten as the following dimensionless equation,

$$1 + \frac{u^2}{2c_p T} = \frac{T_0}{T} \tag{3}$$

If the enthalpy and the temperature tend to zero, the speed reaches a maximum value[9]. Thus, the ratio of velocities is the following,

$$\frac{u}{u_{max}} = \sqrt{\frac{T_0 - T}{T_0}} \tag{4}$$

From compressible flow, it is also known the definition of sound speed a,

$$a = \sqrt{\gamma R T} \tag{5}$$

where $\gamma = c_p/c_v$ (6) is the constant ratio of specific heat capacities (hypothesis vii), c_v the specific heat at constant volume and R the gas constant. The dimensionless Mach number is defined by using the sound speed,

$$Ma = \frac{u}{a} \tag{7}$$

Operating with the previous equations, it is obtained the dimensionless ratio of isentropic and adiabatic flow of an ideal gas,

$$1 + \frac{\gamma - 1}{2} Ma^2 = \frac{T_0}{T} \tag{8}$$

To study its hydraulic analogy, it is considered a reservoir open to the atmosphere of fluid depth H_1 connected to a hydraulic canal. Assuming it is a steady-state flow, the Bernoulli equation can be applied between points 1 and 2[10],

$$P_1 + \frac{1}{2}\rho v_1{}^2 + \rho g H_1 = P_2 + \frac{1}{2}\rho v_2{}^2 + \rho g H_2 \tag{9}$$

where P is pressure, ρ density and H_2 the flow height in any point of the canal. Both pressure terms can be removed by working with gauge pressures, and kinematic energy is approximated to zero since the area of the reservoir is much bigger than the area of the hydraulic canal. Hence, replacing point 1 as the stagnation state H_0 and point 2 as a generic point of height H, the previous equation results,

$$v = \sqrt{2g(H_0 - H)} \tag{10}$$

The maximum fluid velocity is reached when height H tends to zero. Thus, the ratio of velocities is derived again,

$$\frac{v}{v_{max}} = \sqrt{\frac{H_0 - H}{H_0}} \tag{11}$$

After some mathematical manipulations, omitted for the sake of simplification, and taking into account the definition of the dimensionless Froude number, equation (10) can be rewritten as:

$$Fr = \frac{v}{\sqrt{gH}} \tag{12}$$

$$\frac{H_0}{H} = \frac{1}{2}Fr^2 + 1 \tag{13}$$

If equations (4) and (11) are compared, a certain similarity between the ratios of velocities of the two flow types arises,

$$\frac{u}{u_{max}} \sim \frac{v}{v_{max}} \rightarrow \sqrt{\frac{T_0 - T}{T_0}} = \sqrt{\frac{H_0 - H}{H_0}} \rightarrow \frac{T}{T_0} = \frac{H}{H_0} \tag{14}$$

By substituting it in the previous equations (8) and (13), the following expression is obtained,

$$1 + \frac{\gamma - 1}{2}Ma^2 = \frac{1}{2}Fr^2 + 1 \tag{15}$$

At this point the first analogy between Mach and Froude numbers is revealed, if the hydraulic current is seen as a hypothetical gas flow of $\gamma = 2$. As a consequence, both dimensionless numbers can be equally estimated[10].

$$Ma \cong Fr = \sqrt{2\left(\frac{H_0}{H} - 1\right)} \tag{16}$$

Flow analogy with area change

Starting from the equations of perfect gas, isentropic flow and the Continuity equation, an expression that relates Mach number to the surface of a duct and the area change in the flow's direction can be derived. The intermediate and detailed steps can be found in the 6th edition of White's book[9],

$$\frac{A}{A^*} = \frac{1}{Ma}\left[\frac{2}{\gamma + 1}\left(1 + \frac{\gamma - 1}{2}Ma^2\right)\right]^{\frac{\gamma+1}{2(\gamma-1)}} \tag{17}$$

where A is the surface and the superscript "$*$" represents sonic conditions.

The Continuity equation can be applied to a liquid flow in a horizontal open-channel with width variation in the flow direction, resulting in an equation that relates the heights H_0 and H with the volumetric flow rate (Q) and the channel width (b)[10],

$$H_0 = H + \frac{Q^2}{2gH^2b^2} \tag{18}$$

H_0 reaches its maximum value when $H = H^*$; in other words, when the height is under critical conditions. To find this value, equation (18) has to be derived respect to H and make it equal to zero,

$$H^* = \left(\frac{Q^2}{gb^2}\right)^{1/3} \tag{19}$$

By combining equations (18) and (19) results the value of $H_{0,min}$,

$$H_{0,min} = \frac{3}{2}H^* \tag{20}$$

Applying now the Continuity equation between any point of the canal and the point of critical section, and after some algebraic manipulation, it is obtained the ratio of widths of the canal only as a function of Froude number.

$$\frac{b}{b^*} = \frac{1}{Fr}\left[\frac{2}{3}\left(1 + \frac{1}{2}Fr^2\right)\right]^{3/2} \tag{21}$$

If the assumption of the water flow as hypothetical gas of γ=2 is once more taken and applied in equation (17), the hydro-gasdynamic analogy for the ratio of the throat area and the local area in the diffuser is derived,

$$\frac{A}{A^*} = \frac{1}{Ma}\left[\frac{2}{3}\left(1 + \frac{1}{2}Ma^2\right)\right]^{3/2} \tag{22}$$

Additionally, Figure 1 outlines the analogy between the Mach and Froude numbers and their main variables.
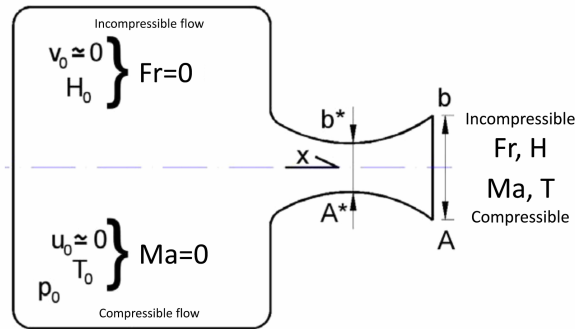
Figure 1. Hydro-gasdynamic analogy with area change diagram

Bidimensional flow analogy

The analogy between bidimensional supersonic compressible flow and supercritical incompressible flow is studied. A shock wave can form an oblique angle when the oncoming flow collides with an obstacle, like a wedge of angle 2θ in Figure 2. Under particular conditions for an incompressible flow, the analogous oblique hydraulic jump arises[4,5,8-10]. Both configurations are depicted in Figure 2.
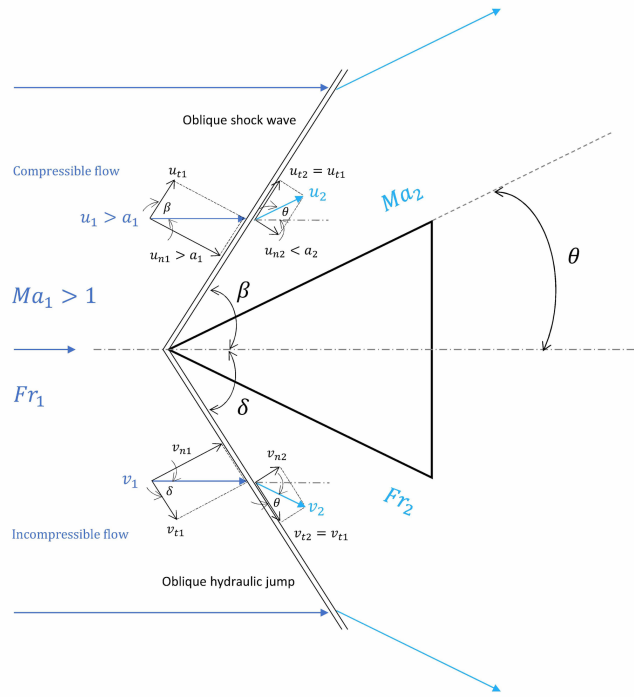
Figure 2. Bidimensional flow analogy diagram

The top part of Figure 2 illustrates the oblique shock wave diagram, where β is the angle between the shock wave and the incident supersonic current. Likewise, subindex 1 refers to supersonic flow, subindex 2 to the flow after the shock wave (subsonic, sonic or supersonic), subindex n to normal components and subindex t to tangential components. The mathematical relation between all these variables[9] is well known as,

$$\theta = tan^{-1}\left[\frac{2cot\beta\left(Ma_1{}^2sin^2\beta - 1\right)}{Ma_1{}^2(1{,}4 + cos2\beta) + 2}\right] \tag{23}$$

The bottom part of Figure 2 exemplifies the oblique hydraulic jump diagram, which is analogue to the one that corresponds to compressible flow. In this case, δ is the angle between the hydraulic jump and the oncoming flow, and the following equation outlines its mathematical relation with the other variables[10],

$$\theta = \delta - tan^{-1}\left[\frac{2tan\delta}{-1 + \left(1 + 8Fr_1{}^2sin^2\delta\right)^{\frac{1}{2}}}\right] \tag{24}$$

Materials and Methods

A detailed experimental set-up was designed (see Figure 3) to study a hydraulic jump and its analogous properties with the compressible flow shock wave. The main components are an upstream plastic reservoir (1 in Figure 3 and see Figure 4), a downstream plastic reservoir (3 in Figure 3 and see Figure 4), a Laval nozzle (2 in Figure 3 and see Figure 4) and three wedges (see Figure 5). The nozzle and wedges were made of polylactic acid (PLA), printed in a 3D printer, and were painted with a waterproof recovering to ensure a higher quality and smooth surfaces. To ensure the maximum resistance, waterproof recovering and the most uniform finish, a sheet of plastic was also placed above the canal's base. Both reservoirs have twenty-five litres of capacity and the nozzle's length is around half a meter, so that the volume of the whole installation does

not exceed one cubic meter. These dimensions were set as a requirement of the project to make the assembly fit in any classroom with space limitation.
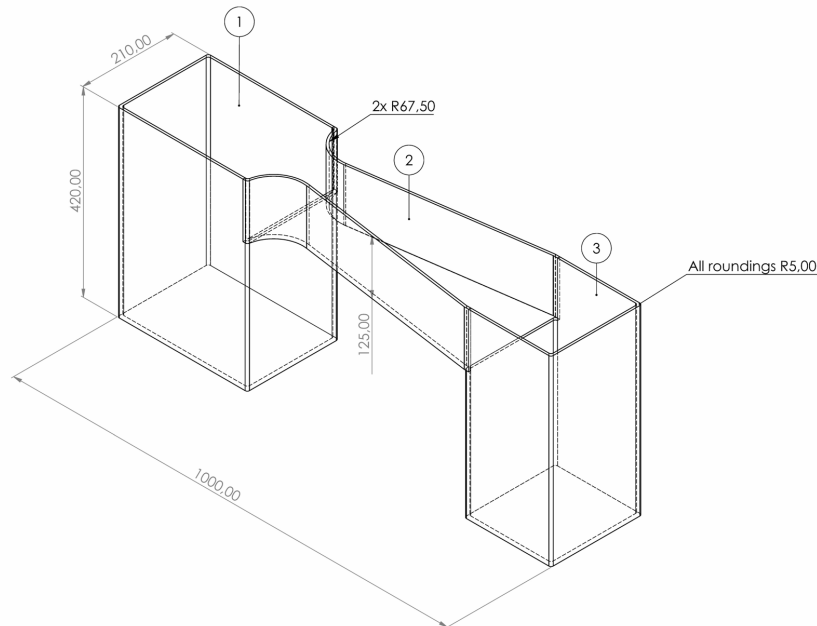
Figure 3. Baseline 3D design and architecture of the experimental equipment

The final design selected came from an extensive process of evaluating alternatives made of different materials, such as methacrylate or stainless steel. However, these materials would have needed the assistance of a professional manufacturer, which it would have significantly raised the cost. In addition, the constructed set-up shown in Figure 4 operates on a very low budget compared to a supersonic wind tunnel[8].

Other elements were added in order to facilitate the whole set-up to achieve its objective, as shown in Figure 4. The hydraulic circuit starts with a water pump, from which it reaches the upstream reservoir through valves and pipes that regulate the volumetric flow. At this point, an optional filter can be located in order to steady the regime and remove all possible flow stirring, as well as ensuring a subcritical water flow entering the nozzle. Through the nozzle throat, the flow accelerates achieving first the critical state and finally the supercritical one. Then, the hydraulic jump makes the water return to its slow subcritical regime. For a better visualisation of all these changes in the water's movement, some patterned templates were placed in the test section, illuminating them from above with a lamp. Other visualisation methods were considered, although the results were of minor significance. Additional items were also tacked on to enable the gathering of data; a slide gauge was used to precisely measure the upstream and downstream heights, a graduated cylinder and a chronometer worked for gathering the volumetric flow, and a pair of adjustable plates were modulated to vary the width of the throat.
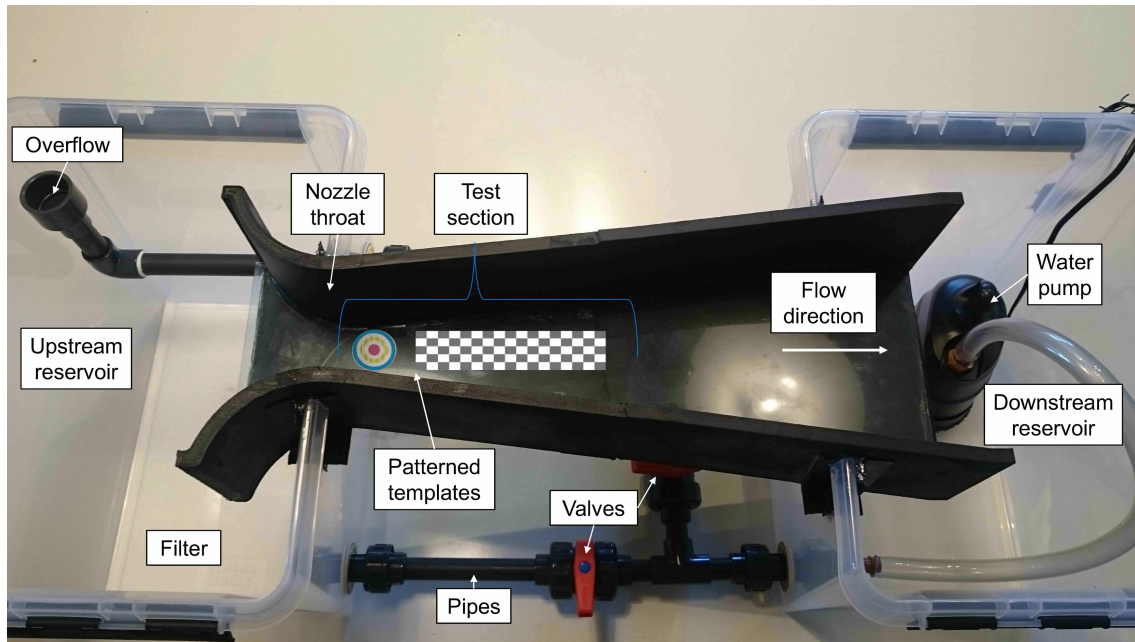
Figure 4. In-house low-cost experimental set-up

By contrast, to visualise an oblique hydraulic jump, an obstacle had to be placed in the path of the water. Three wedges of angles 7.5°, 15° and 20° were designed with a height of 0.04 m and a length of 0.08 m to ensure and enhance the visualisation of the oblique hydraulic jump and also to fit the nozzle's dimensions (see Figure 5).
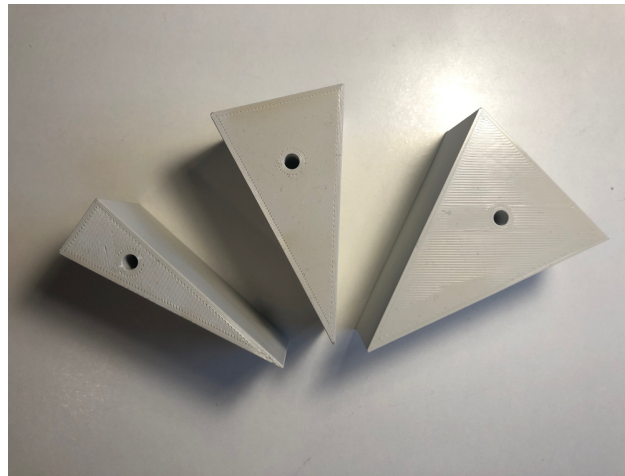

Figure 5. Wedges of 7.5°, 15° and 20°

Procedure

Figure 6 depicts the main variables to take them into account in the methodology description and in the standard test procedure. There are two independent variables: e, the width of the throat, and b, the width of the nozzle's diffusing part. The width of the throat was adjusted from 0.07 m to 0.03 m in steps of 0.01 m by means of the adjustable plates. Each of these widths generated a specific Froude number, which could be analytically obtained through the measured heights H_0 and H, shown previously in equation (16). Therefore, these heights can be defined as the dependent variables of the experiment. Finally, b was used to fix the point of the nozzle's diffusing ending part, right after the hydraulic jump occurred. The value of 0.085 m was

established constant in all cases, in order to simplify the procedure and after having checked that from this point did not vary the height of the downstream flow. The significance of this width comes from obtaining theoretically the area ratio A/A* by dividing b by $b^*(= e)$, whereas the experimental ratio A/A* can be calculated through equation (22). Figure 6 shows the relationship between all these variables.

The volumetric flow was evaluated for each width in order to obtain an experimental value of the Froude number by using equation (12). It is a second approach used to verify the correct functioning of the experiment and the creation of a hydraulic jump.
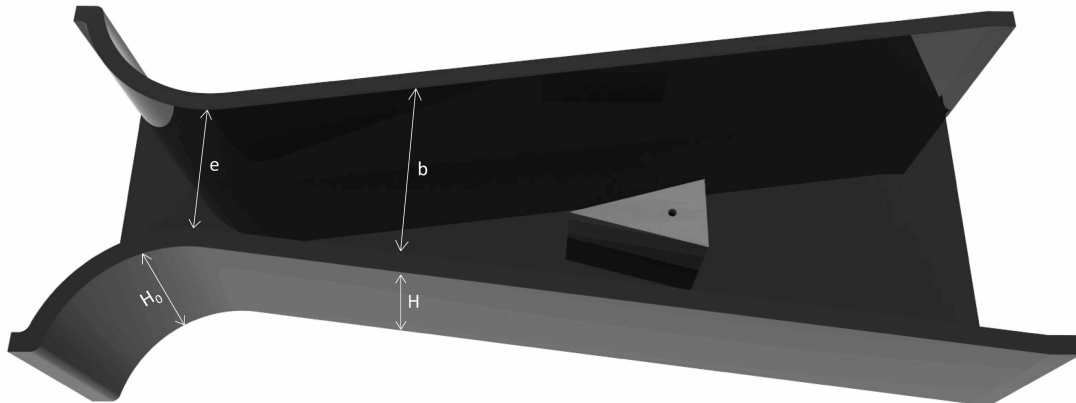
Figure 6. Variables of the first stage of the experiment

The independent variables of the second stage of the experiment are also the widths e and b, by adding the angle of the wedges θ. Hence, the angle of the oblique hydraulic jump δ caused in each case is the dependent variable (see Figure 7). The wedges were placed at three widths of the throat: 0.07 m, 0.06 m and 0.05 m.
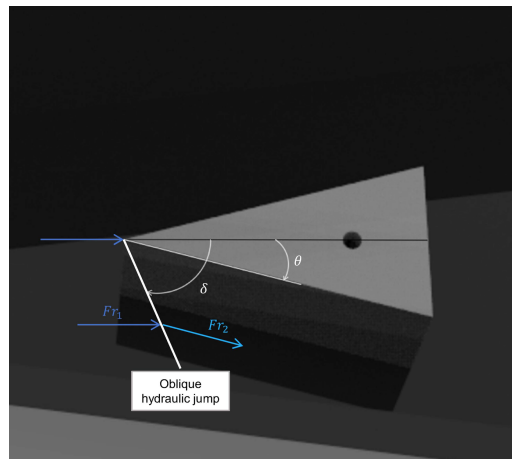
Figure 7. Variables of the second stage of the experiment

Results

i.   Normal hydraulic jump

The propagation of error analysis was obtained according to Coleman and Steele[11]. The uncertainty of heights, volume and time were 0.00001 m, 0.02 L and 0.01 s, respectively. The

maximum uncertainty values of Mach and Froude numbers were 0.002 and 0.039, respectively. The uncertainty in each of the fluid properties was estimated to be lower than 1%.

For each of the fixed five widths of the nozzle's throat, two Froude numbers were calculated from equations (12) and (16), respectively. To illustrate its significance, they are represented in a graphic by parameterising the independent variable e as shown in Figure 8. The figure also deals with variability and depicts the error bars.

Equivalent data treatment of the theoretical and experimental values of A/A* was carried out for each nozzle's throat width (see Figure 9), although the error bars are so small that are barely noticeable.
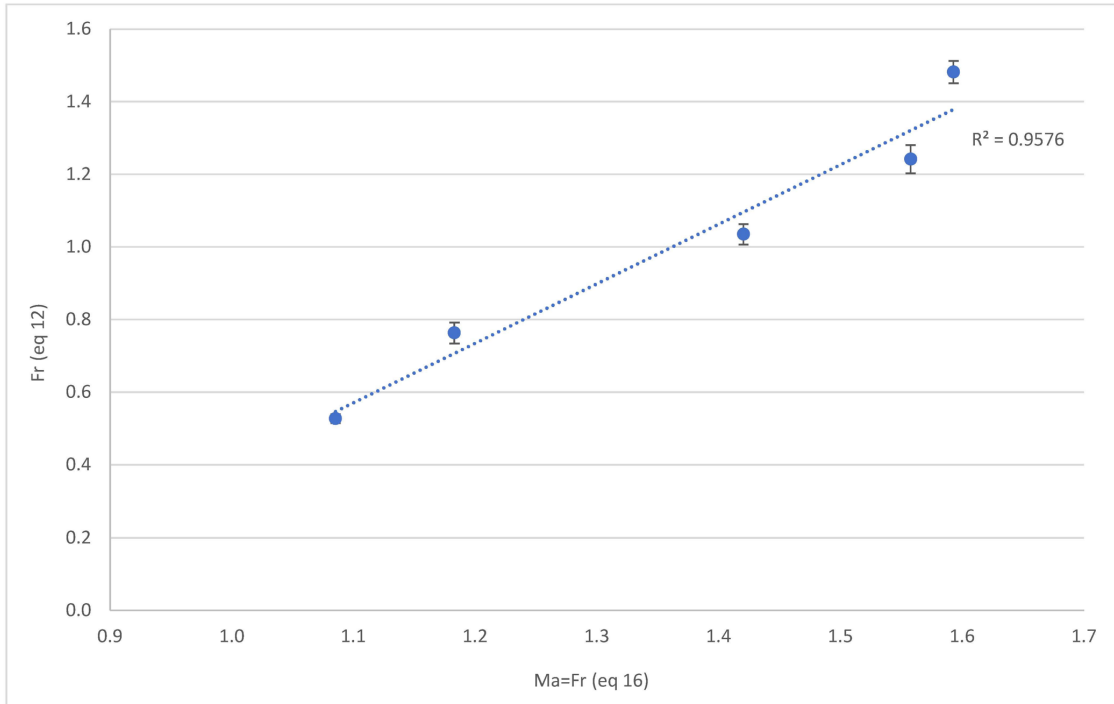
Figure 8. Linear regression of the parameterised Froude numbers as a function of the nozzle's throat width (first stage of the experiment)
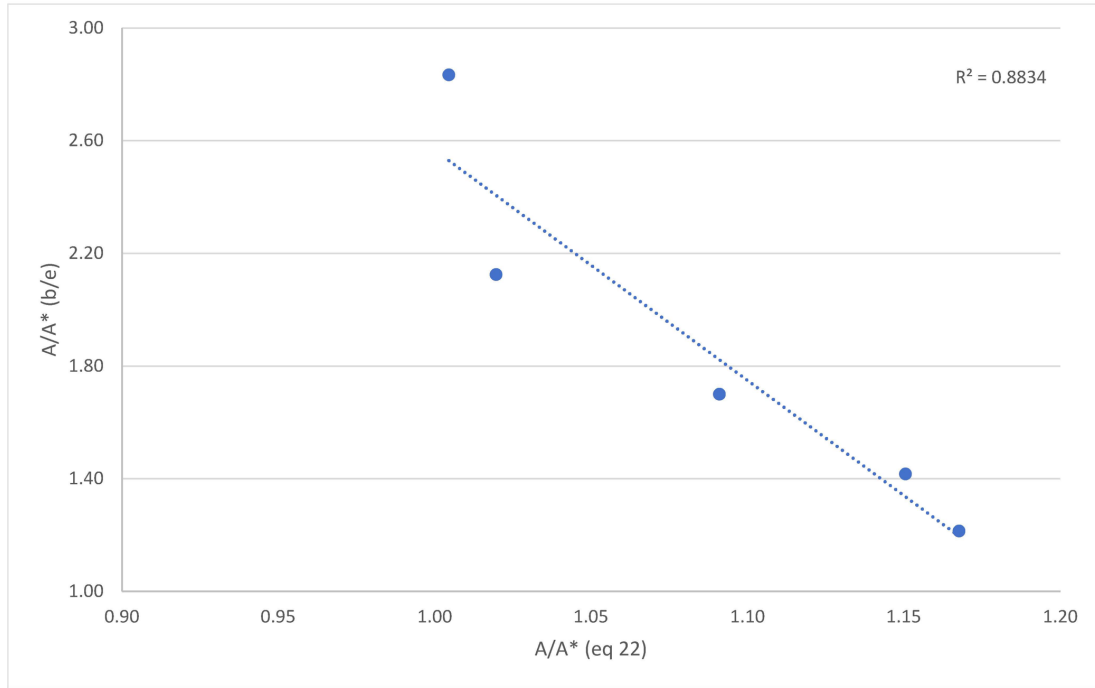
Figure 9. Linear regression of the parameterised A/A* as a function of the nozzle's throat width (first stage of the experiment)

Photo tracking was also utilised as a means to physically capture the hydraulic jump. Figure 10 shows an example of it when the width of the throat is 0.05 m.


Figure 10. Examples of a hydraulic jump and the adjustable plates

ii.   Oblique hydraulic jump

The theoretical analysis, the hydro-gasdynamic analogy and the first stage of the experiment showed that the best results were obtained from the throat widths of 0.07 m, 0.06 m and 0.05 m. For nozzle throat widths above 0.04 m, Froude numbers from equation (12) were higher than one, denoting that the supercritical regime was reached. Only those cases revealed the generation of a hydraulic jump along with more accurate results. According to that, the second stage of the experiment was conducted to measure nine cases, and in five of them was possible to see experimentally an angle δ of the oblique hydraulic jump. None of them was from the wedge of 20°, as it was also previously shown by Goushcha for low values of supercritical Froude numbers[4].

11

Heights H_0 and H were also measured in order to obtain Froude numbers (through equation (16)) and consecutively theoretical δ values from equation (24), calculated by using MAPLE™ program[12]. Nevertheless, these theoretical values revealed that for the wedge of 15° the oblique hydraulic jump did not materialise. Analogous to the behaviour of compressible flow, it occurs a detached shock wave (DS). This means that under these conditions, angle θ and Froude number, a δ value between 0 and 90° does not exist.

Froude numbers were also obtained from equation (12), as in the first stage of the experiment, being possible to represent a linear regression as illustrated in Figure 11.
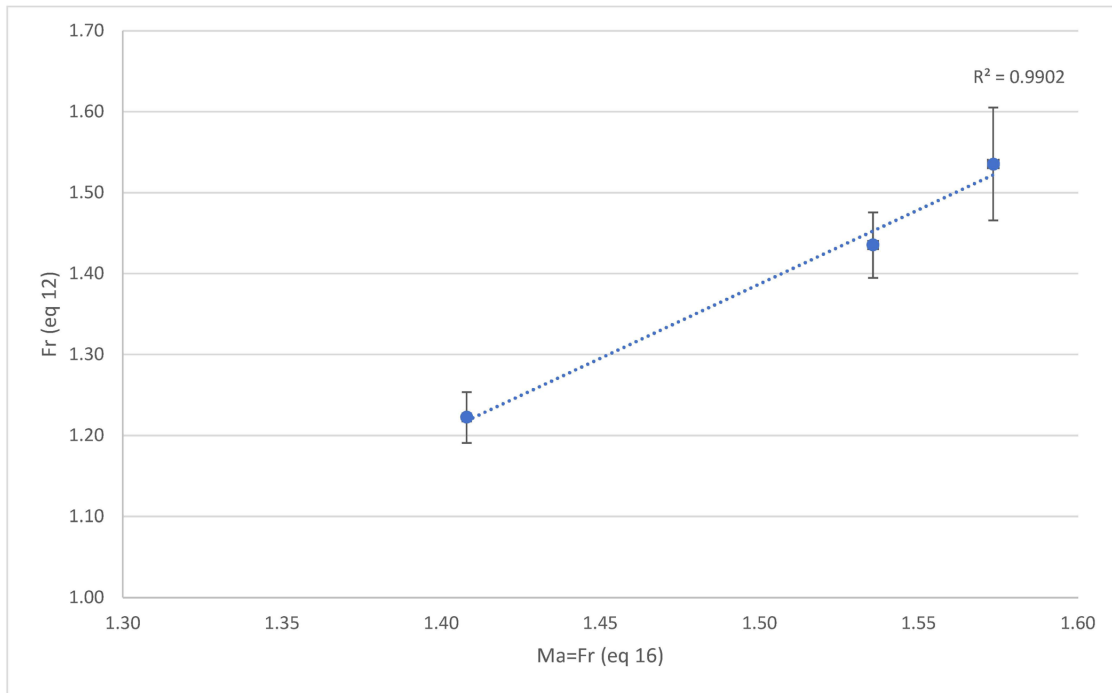
Figure 11. Linear regression of the parametrised Froude numbers as a function of the nozzle's throat width (second stage of the experiment)

In order to enhance comprehension, Figure 12 depicts two experimental examples. The first experiment corresponds to a throat width of 0.07 m and a wedge of 7.5°, where clearly occurs an oblique hydraulic jump. The second experiment corresponds to a throat width of 0.05 m and a wedge of 20°, where no oblique hydraulic jump can be visually distinguished.

Figure 12. Left) Example of an oblique hydraulic jump; Right) Example of a detached shock wave

Discussion

Given the difficulties presented in the production of a hydraulic jump, it should be pointed out the achievement of having obtained Froude numbers greater than one, from equation (16), as it means having reached the supercritical regime. Additionally, the fact that an undular jump was visually detected and recorded (see Figures 10 and 12), together with the significant agreement according to the theoretical framework, is outstanding, in spite of not having looked for a professional manufacturer's help. Not only was this possible weakness addressed, but also it added value to the results obtained from the ad-hoc low-cost experimental set-up.

If Figure 8 is observed, it can be seen that Froude numbers from equation (12) are greater than one only for nozzle throat widths above 0.04 m, which indicates the experimental formation of a hydraulic jump for this range of width values. This result is consistent with the fact that the error between the results from both equations increases when the width decreases, from 7% ($e = 0.07$ m) to 51% ($e = 0.03$ m).

Regarding the analysis of Figure 9, and comparing the experimental results of A/A* with the theoretical ones, the previous conclusion is confirmed as the error between values increases again when e decreases. Particularly, the error between measures goes from a 4% ($e = 0.07$ m) to a significant 65% ($e = 0.03$ m). In past experimental studies on the same topic, the error also grew when the throat width was reduced, so that it gives credibility to the results obtained in this work[3]. Consequently, the interpretation of this study concurs with the one developed by experts of other universities[4,8].

In addition, when the angle of the nozzle is higher, making its width smaller, the probability of what it could be called "stall" becomes higher, and this phenomenon can produce alterations in the flow path[13]. From the nozzle geometry designed in this experimental study, the theory confirms the presence of a "two-dimensional stall" for width values lower than 0.05 m, which would justify the high error values. Hence, a plausible explanation is that hydraulic jump occurs for wide widths, whereas stall can appear as a restriction for narrow widths.

According to the results of the second stage of the experiment and equation (24) from the theoretical framework, it can be outlined that the wedge of 7.5° produced a prominent oblique hydraulic jump in the manufactured experimental set-up. The trial with less error was given for the width of 0.06 m, 5%, and the greatest for the width of 0.07 m, 20%. The source of this major error is based on the fact that for a higher Froude number, the tendency that should follow the angle δ is to decrease and not to grow. This trend was fulfilled in the other two cases, but not in the first one. Although the behaviour of each δ value corresponding to a throat width differed, Froude numbers did follow a similar tendency as depicted in Figure 11 with a high coefficient of determination (0.99) resulting from its linear regression.

It is worth mentioning that the low values of the error bars shown in the graphical results are due to the good resolution of the equipment used. Only in Figure 11 error bars can be perceived at a higher size, but that is because the scale used is smaller in order to gain comprehension.

Finally, this study found the cause-and-effect relationship between the results obtained and their meaning, which brings a sense of fulfilment. Despite the difficulties and low budget invested, the presented work proves valuable.

Conclusion

This paper provides a detailed explanation of the design and manufacture of an in-house ad-hoc low-cost water table. From the theoretical study and experimental data obtained, it is concluded that under the suitable boundary and geometrical conditions, a compressible flow in a water table can be modelled on hydro-gasdynamic analogy. Then, the main goal of illustrating hydro-gasdynamic analogy with a hydraulic jump has been accomplished. Despite it being difficult to physically visualise it in some cases, the theoretical analysis has been successfully confirmed.

The measurements have shown that the greatest nozzle throat width, 0.07 m, achieves the best agreement between theoretical and experimental values based on Froude numbers and ratios of the throat and the local area in the nozzle. For nozzle throat widths above 0.04 m, Froude numbers were higher than one, denoting that the supercritical regime was reached.

The main encountered errors in the measurements were caused when the width of the throat decreased, which foments the flow "stall" from the walls and were enhanced when the nozzle's angle increases. Hence, the hydraulic jump occurs for wide widths, whereas stall can appear as a restriction for narrow widths. Then, it is of interest for a future investigation to design a nozzle of higher experimental widths, to try to reduce this phenomenon and better visualise the hydraulic jump.

The oblique hydraulic jump was more easily detected visually than the normal hydraulic jump. Of the three wedges used to cause obliquity, the deflection angle produced by the wedge of 7.5° led to better results. Not only did its measurements reduce errors, but it also avoided causing any analogue detached shock wave.

This work promotes commitment and learning stimulation: the more practice students are provided with, the more interested they become in the field. Despite the encountered limitations of the hydrodynamic analogy and the simplicity of the designed lab apparatus, particularly in the supercritical regime and oblique hydraulic jump, it provides an opportunity to carry out lab experimental measurements, which certainly leads to a better understanding of fluid mechanics. In addition, compressible flows are not common in nature and it is challenging to make them visible with the naked eye, and then expensive technical equipment is required. Definitely, it is more illustrative and formative to physically see results with a theoretical background rather than memorising random formulas.

ORCID ID

Sílvia Armengol   https://orcid.org/0000-0001-8875-6950

Gustavo Raush   https://orcid.org/0000-0002-9730-5091

Pedro J Gamez-Montero   https://orcid.org/0000-0002-5168-3521

References

1. Shapiro A. H. *The Dynamics and Thermodynamics of Compressible Fluid Flow* (Vol. 1). NY: Ronald Press, 1953.
2. Anderson J. *Modern Compressible Flow With Historical Perspective* (Third ed.). NY: McGraw-Hill, 2003

3. Goushcha O. Revival of water table experiments in fluid mechanics, part I. *International Journal of Mechanical Engineering Education* 2019; 48(3), 284−293.

4. Goushcha O. Revival of water table experiments in fluid mechanics, part II. *International Journal of Mechanical Engineering Education* 2020.

5. Elward KM. *Shock formation in overexpanded flow: a study using the hydraulic analogy* (Doctoral dissertation, Virginia Tech): 1989.

6. Garretson IC, Torner FM, Seewig J and Linke BS. An algorithm for measuring the hydraulic jump height of an airfoil in a water table. *Measurement* 2019; 148.

7. Morishita E. Compressible pipe flow and water flow over a hump. In *Proceedings of the World Congress on Engineering* 2013; 3, 1−4.

8. Pouderoux P. Master of science thesis: *water table analogue for compressible flow studies.* Corvallis, OR:Oregon State College, 1953.

9. White FM *Fluid Mechanics* (Sixth ed.). NY: McGraw-Hill, 2008

10. Morishita E. Compressible pipe flow and water flow over a hump. *International Journal of Aerospace and Mechanical Engineering* 2018; 12(12), 1092−1105.

11. Coleman HW and Steele WG. *Experimentation and Uncertainty Analysis for Engineers*. NY: John Wiley & Sons, 1999.

12. Maple Programming Guide. L. Bernardin, P. Chin, P. DeMarco, K. O. Geddes, D. E. G. Hare, K. M. Heal, G. Labahn, J. P. May, J. McCarron, M. B. Monagan, D. Ohashi, S. M. Vorkoetter. Maplesoft, a division of Waterloo Maple Inc., 1996-2021.

13. Reneau, L. R., Johnston, J. P., & Kline, S. J. (1967). Performance and Design of Straight, Two-Dimensional Diffusers. Journal of Basic Engineering. Retrieved 06 08, 2021, from https://sgp1.digitaloceanspaces.com/proletarian-library/books/5378296e745e8101666527285ae257da.pdf.